

N 7 2 - 2 6 9 7 0

**NASA TECHNICAL
MEMORANDUM**

NASA TM X-68075

NASA TM X- 68075

**CASE FILE
COPY**

**IDENTIFICATION OF BOILER INLET TRANSFER FUNCTIONS
AND ESTIMATION OF SYSTEM PARAMETERS**

by Jeffrey H. Miles
Lewis Research Center
Cleveland, Ohio

TECHNICAL PAPER proposed for presentation at
1972 Joint Automatic Control Conference sponsored
by the American Institute of Aeronautics and Astronautics
Stanford, California, August 16-18, 1972

IDENTIFICATION OF BOILER INLET TRANSFER FUNCTIONS AND ESTIMATION OF SYSTEM PARAMETERS

Jeffrey H. Miles

Lewis Research Center
National Aeronautics and Space Administration
Cleveland, Ohio

Abstract

An iterative computer method is described for identifying boiler transfer functions using frequency response data. An objective penalized performance measure and a nonlinear minimization technique are used to cause the locus of points generated by a transfer function to resemble the locus of points obtained from frequency response measurements. Different transfer functions can be tried until a satisfactory empirical transfer function of the system is found. To illustrate the method, some examples and some results from a study of a set of data consisting of measurements of the inlet impedance of a single tube forced flow boiler with inserts are given.

Introduction

Studies of the dynamic stability of single tube boilers have been conducted at the NASA Lewis Research Center. The aim of these studies was to establish dynamic system stability criteria. The experimental part of the program consisted of measuring the frequency response of the system.^(1,2,3) As part of the analytical program a method was developed to identify transfer functions from these measurements. This report presents the details of this method. Typical results obtained by applying the method to the boiler frequency response data are also presented.

The frequency response data consist of the amplitude ratio and the phase angle difference of two parameters at various frequencies. The frequency response is considered to be identified if a transfer function that fits the frequency response data is obtained. Various approaches can be used to analyze these data to obtain a satisfactory transfer function.

If nothing were known about the dynamic system, a heavily empirical approach could be adopted. For example, it could be assumed that the system transfer function is composed of pure time delays e^{-T_i} , gains k_i , and associated time constants τ_i . It could further be assumed that the transfer function Z had the general form

$$Z(s) = \sum_{i=1}^N \frac{k_i e^{-T_i}}{1 + \tau_i s}$$

where $s = j\omega$. This curve fitting approach does not have generality. The constants are not related by theory to the steady-state condition and must be calculated for each test measurement.

Another approach to the problem would be to attempt a rigorous solution of the partial differential equations governing the boiler. This approach assumes all important processes are known.

The approach taken herein was to develop a method that could yield an analytical model. The method is used to obtain a transfer function with the following characteristics: The transfer function should describe the measured data; the transfer function should preferably be derivable from a physical theory; and the dimensionless gains, time delays, and time constants in the transfer function should be derivable from steady-state measurements or physical properties. This report is concerned with the development of the method and not with relating results to fundamental physical principles.

In the next section the general method is explained. In the then following section, the results of applying the procedure to boiler inlet impedance measurements are given. The last section contains a further discussion of this work.

Method

The success of the method is determined partially by the extent the locus of points generated by the transfer function (LPG) resembles the locus of points obtained from frequency response measurements (LPM). The locus of points in either case is obtained by connecting the frequency response points in the order of increasing frequency. While it is necessary that this resemblance criterion be satisfied, resemblance is not a directly measurable quantity. A secondary criterion called an objective performance measure is used to provide a quantity that is directly measurable.

A description of the manner in which this performance measure is used to investigate resemblance between LPM and LPG follows. Each physical description (based on experimental results or fundamental physical principles) thought to describe the fundamental dynamic phenomena is used to produce a system transfer function corresponding to the one measured.

Each physical description yields estimates of the gains, time delays, or time constants in the transfer function. It also yields information on the possible ranges for these constants. For each transfer function the constants are selected to minimize the positive, quadratic performance measure. The form of the performance measure used also ensures that all the constants will be within their proper limits. In this manner each analytical model can be compared to measured frequency response data.

The objective performance measure indicates which physical description is most applicable. The best LPG can be checked for resemblance by plotting and comparing with the LPM.

In this manner a transfer function is constructed by an iterative procedure. At each step the results can suggest modifications in the analysis that are necessary for improvement. This pro-

cedure can be used to pinpoint the inadequacies in an analysis.

The basic performance measure S is

$$S = \sum_{i=1}^N \left[|Z(s_i, x) - Z_{\text{obs}}(s_i)| \right]^2$$

where $s_i = j\omega_i$ and the $\{x\}$ are the transfer function constants. The performance measure is the sum of the square of the magnitude of the separation of the measured impedance Z_{obs} and the calculated impedance Z at all frequencies where measurements are made. Previous reports (4,5,6) have suggested that a determination of the approximate system transfer functions and parameters can be made by finding the transfer function constants which minimize the performance measure. Standard computer techniques, to be discussed later, are used to find the constants $\{x\}$ which minimize the performance measure.

The actual performance measure used herein was a modified form of the previously given basic definition. First, the basic performance measure S was changed to a weighted performance measure S_w . This was done for various reasons. The weighted performance measure provides a simple means to obtain a performance measure that applies over a limited frequency range. As an example, if measurements were made over a range from 0.001 to 4.0 hertz and if only the range from 0.001 to 1 hertz was to be covered by the transfer function, the weighting factors for frequencies larger than 1 hertz could be set to zero. The weighted performance measure furthermore provides a simple way to minimize the effects of noise or of errors on the identification procedure. It also provides proper scaling. The weighted performance measure has the form

$$S_w(k, m) = \sum_{i=1}^N \alpha(k, m)_i \left[|Z_k(s_i, \{x(m)\}) - Z_m(s_i)| \right]^2$$

The k index represents the k^{th} theory. The m index represents the m^{th} set of data. The weighting factor is designated as $\alpha(k, m)_i$.

Since the selection of values of the transfer function constants is automated, one further modification was made to the performance measure. This modification was made to insure that the constants selected in minimizing the performance measure are in the proper range. The estimates of the proper range for each constant are used to provide constraints on the selection of parameters, and an acceptable variation of parameters is obtained. Hence, a transfer function need not be discarded if the initial selection of parameters was incorrect. An adequate understanding of the process or a lack of knowledge of important steady-state parameters need not prevent the recognition of a suitable transfer function if the range of the parameters can be estimated.

The selection of parameters was constrained by the penalty function

$$[p_l(x) = d(k, m)_l - x(k, m)_l]^2 \delta_l$$

where

$$\delta = \begin{cases} 0 & \text{for } x(k, m)_l < d(k, m)_l \\ 1 & \text{for } x(k, m)_l > d(k, m)_l \end{cases}$$

This penalty function has the following characteristics. If the estimated parameter $x(k, m)_l$ for the k^{th} theory and m^{th} steady-state condition is less than the estimated constraints, the penalty p is zero. If the estimated parameter $x(k, m)_l$ is greater than the estimated constraint, the penalty is equal to the square of the difference between the penalty and constraint. The penalty due to these individual penalty functions was defined as the weighted sum of these penalty function.

With this penalty function, the objective performance measure S_p was defined to be

$$S_p(k, m) = S_w(k, m) + \sum_{i=1}^N w_i p_i(x)$$

The weighting factor w_i is selected to scale the penalty p_i such that each penalty will have an appropriate effect on S_p .

The problem of minimizing a nonlinear function like the performance measure can be solved by a search technique. The basic methods available are discussed in chapter 6 of Ref. 7. To provide maximum flexibility in the choice of Z , a search technique which does not require evaluation of derivatives was chosen. The search technique used was that of Powell.(8) The computer program used was adapted from Ref. 9.

When the penalized performance measure and the computer methods mentioned previously are combined, the computer method shown schematically in Fig. 1(a) results. This method is used to find out if a particular choice of transfer function fits the measured frequency response data.

The procedure used to obtain a satisfactory transfer function is shown in Fig. 1(b). Only the step in which $S_p(k, m)$ is calculated is programmed on the computer. For the first transfer function it is best to select one based on a simple first-order theory that yields an approximation to the LCFM and that uses the steady-state data available to predict the transfer function constants and constraints. At this point it is best to select the data that are easiest to work with and to limit the frequency range over which agreement is expected. This initial transfer is denoted as Z_1 . The set of parameters obtained is denoted as $\{x(1, m)\}$ and the set of constants is $\{d(1, m)\}$. The minimum value of $S_p(1, m)$ can then be found. It should be noted that in this expression S_p^* may be minimized to yield a transfer function Z_1^* which is optimum over a limited frequency range.

For the following iterative steps it is necessary to examine previous results to locate terms that would extend the frequency range, terms that would enable the theory to be extended to more steady-state operating conditions, and terms that were not used because of insufficient steady-state knowledge or physical knowledge. After the functional form of these neglected terms is found, the value of the parameters in these terms and the constraints on these parameters are then estimated.

These terms when combined together produce various theoretical transfer functions. The k^{th} theoretical description yields transfer function Z_k . Also from the k^{th} theoretical description and for each steady-state condition, a set of constants $\{x(k,m)\}$ and a set of constraints $\{d(k,m)\}$ are available. The minimum value of $S_p(k,m)$ is found. The resulting set of optimized transfer functions Z_k^* is compared.

The results of each change in the theoretical transfer function, change in frequency range, or change in constraints on the previous theoretical transfer function are readily available using the computer method.

The procedure described previously was used to obtain a transfer function for the inlet impedance of a single tube, forced flow boiler with inserts from inlet impedance measurements. The following section discusses some of the results of this work. The aspects discussed in the next section are those not concerned with relating the transfer function obtained to a set of fundamental physical principles.

Application

This section initially indicates how the contributions of various transfer functions (each attributed to a different physical process) are separated in the formulation of the system transfer function. This is done so that each can be considered independently. The transfer function for one process can then be changed until the system transfer function is improved while maintaining the transfer functions for other processes constant. Next, some typical results obtained by using the performance measure, computer techniques, and the iterative procedure described in the previous section are given. Last, the transfer functions which were found by this method are discussed.

The analyzed data⁽²⁾ were obtained experimentally by driving sinusoidally the open area of a valve in the feed system about a mean area and measuring the pressure and flow at the boiler inlet. The pressure and flow signals were analyzed by a frequency-response analyzer. This analyzer computed the magnitude and phase of the sinusoidal content of the pressure and flow signals at the driving frequency. The magnitude of the boiler inlet impedance at each frequency is equal to the amplitude ratio of the inlet pressure to inlet flow signals. The phase of the boiler inlet impedance at each frequency is equal to the difference between the measured phase angle of inlet pressure and inlet flow.

The theoretical model used to describe the measured boiler input impedance data is a function of a combination of physical processes. The different physical processes are assumed to be tied together by a set of equations. While the detailed models of each physical process are not known adequately, the set of equations which forms the framework that ties the models together is assumed to be known.

The equations and subsystem transfer functions are derived from the governing equations for the boiler by (1) simplifying and linearizing for small perturbations about a known steady-state operating condition, (2) Laplace transforming the equations,

and (3) putting the equations in dimensionless form. The dimensionless form is obtained by dividing by scale factors \bar{P} and \bar{W} . The scale factors are not defined individually since in the final equation they appear as \bar{W}/\bar{P} . The quantity \bar{P}/\bar{W} is defined to be 3.28×10^6 newtons-seconds per square meter - kilogram. The result is a set of equations connecting perturbations in parameters. The coefficients of the parameters are the subsystem transfer functions. Each subsystem transfer function represents a physical process.

The perturbation parameters chosen to describe the inlet impedance are the following: the variation of inlet pressure ΔP_{in} , the variation of inlet mass flow rate ΔW_{in} , the variation of vapor pressure beyond the subcooled region ΔP_{Lsc} , the variation of subcooled length ΔL_{sc} , and the variation in vapor mass flow rate beyond the subcooled region ΔW_{Lsc} .

These five perturbations are connected by the following four equations:

$$\frac{\Delta P_{in}}{\bar{P}} = E(s) \frac{\Delta W_{in}}{\bar{W}} + \frac{\Delta P_{Lsc}}{\bar{P}} \quad (1)$$

$$\frac{\Delta L_{sc}}{\bar{L}_{sc}} = G(s) \frac{\Delta W_{in}}{\bar{W}} + H(s) \frac{\Delta P_{Lsc}}{\bar{P}} \quad (2)$$

$$\frac{\Delta W_{Lsc}}{\bar{W}} = \frac{\Delta W_{in}}{\bar{W}} - \theta_2 s \frac{\Delta L_{sc}}{\bar{L}_{sc}} - F(s) \frac{\Delta P_{Lsc}}{\bar{P}} \quad (3)$$

$$\frac{\Delta P_{Lsc}}{\bar{P}} = R \frac{\Delta W_{Lsc}}{\bar{W}} \quad (4)$$

Equation (1) relates the perturbation in pressure drop across the subcooled region to the inlet mass flow rate through an inertial term $E(s)$. Equation (2) states the following:

1. Changes in subcooled length (for constant vapor pressure) are due to perturbations in inlet mass flow rate effecting heat transfer (the transfer function for this physical process is represented by the term $G(s)$).

2. For constant inlet mass flow, perturbations in vapor pressure effect the subcooled length (the transfer function for this physical process is represented by the term $H(s)$).

3. These two effects can be added for small perturbations. Equation (3) states that changes in mass flow rate can be related to mass storage through changes in subcooled length (represented by the term $\theta_2 s$) and in pressure (represented by the term $F(s)$). Equation (4) relates variations in exit flow and exit pressure by the constant R .

The inlet impedance derived using these equations is

$$Z(s) = \frac{\Delta P_{in}/\bar{P}}{\Delta W_{in}/\bar{W}} = \frac{R(1 - \theta_2 s G(s))}{[1 + R \{ \theta_2 s H(s) + F(s) \}]} + E(s) \quad (5)$$

The basic block diagram for the system is shown in Fig. (2).

Each subsystem transfer function and thus each separate physical process can be investigated independently by proceeding in the previously stated manner. Thus, different theoretical models for each physical process can be checked. Also, different mathematical forms of the subsystem transfer functions can be tested. These forms can be those determined from physical theory or from transfer function plots.⁽¹⁰⁾ The method of this report was then used to determine the subsystem transfer functions $G(s)$, $E(s)$, $H(s)$, and $F(s)$. In the following section the results of a study of data taken at a condition of high vapor exit quality are discussed.

High Quality Vapor Exit Condition

The case discussed is run 4 from Ref. 2. The data were obtained at a steady-state condition of high vapor exit quality (99 percent). The boiler inlet impedance data are plotted in Figs. 3(a) and (b). Figure 3(a) contains the data measured over the frequency range 0.04 and 1.0 hertz, and Fig. 3(b) contains plots of the data over the frequency range 0.25 to 4.0 hertz. The basic characteristic form is that of a spiral. Over the frequency range below 1 hertz (fig. 3(a)) the amplitude of the transfer function decreases as the phase angle rotates clockwise. Above 1 hertz (fig. 3(b)) three important changes in the form occur. Between 1.6 and 2.5 hertz a small loop occurs. Beyond 2.5 hertz after the small loop the following loop is larger. Also above 4 hertz the data are not symmetric about (0,0). Instead, the data are symmetric about a line through the real axis. Also, the spiral seems to be pulled up along a line parallel to the imaginary axis. Several theories are now compared with the data.

Theory 1. - The initial transfer function used to provide the starting point in the iterative model building process was the theoretical model described in Ref. 11. This model is designated as theory 1. This theory, which is based on many simplifying assumptions, provides an adequate estimate of the boiler impedance over a limited frequency range for those steady-state conditions where the theoretical simplifications agree with the actual steady-state conditions. The theory was not meant to be applicable to data taken at a condition of very low exit quality or very high exit quality.

The model described in Ref. 11 used the following functional forms for the subsystem transfer functions $G(s)$, $E(s)$, $H(s)$, and $F(s)$:

$$E(s) = x_4 s \quad (6a)$$

$$G(s) = \frac{1 - e^{-\theta_2 s}}{\theta_2 s} \quad (6b)$$

$$H(s) = x_2 \quad (6c)$$

$$F(s) = 0 \quad (6d)$$

The time constant θ_2 is the subcooled dead time and is given by

$$\theta_2 = \frac{L_{sc} \rho A}{\bar{W}} \quad (7)$$

The time constant θ_2 is designated as constant x_1 . The time constant x_4 corresponds to the inertia of the subcooled fluid. It is given in the dimensionless form used here as

$$x_4 = \frac{L_{sc}}{A} \frac{\bar{W}}{P} \quad (8)$$

The gain x_2 corresponds to the change in subcooled length with a change in vapor pressure. In nondimensional form it is

$$x_2 = \frac{\partial L_{sc}}{\partial P_{L_{sc}}} \frac{\bar{P}}{L_{sc}} \quad (9)$$

The boiler resistance previously denoted R is henceforth defined as a constant:

$$x_3 = R \quad (10)$$

To obtain a form of the inlet impedance equation that is more clearly related to more common forms, the following transformation of Eq. (5) was made. Using Eq. (10) and defining

$$QUA = 1 - x_1 s G(s) \quad (11)$$

give

$$Z = \frac{x_3 QUA}{1 + x_3 x_1 s H(s) + x_3 F(s)} + E(s) \quad (12)$$

The first transfer function used in the procedure diagrammed in Fig. 1(b) was derived from Eqs. (11) and (12) and Eqs. (6a) to (d). The result is

$$Z = \frac{x_3 e^{-x_1 s}}{1 + x_3 x_2 x_1 s} \quad (13)$$

Note that from Eq. (11) and (6d)

$$QUA_1 = e^{-x_1 s} \quad (14)$$

Coefficients for this model were selected using the method described in the first section. The resulting function is plotted for frequencies less than 0.3 hertz in Fig. 3(c) and for frequencies greater than 0.3 hertz in Fig. 3(d). Examination of Fig. 3(c) shows that this model does describe the data in the range below 1 hertz. The data and the theory 1 locus both resemble a spiral. The amplitude of the transfer function decreases as the phase angle rotates clockwise. Examination of Fig. 3(d) shows that theory 1 fails in the frequency range above 1 hertz. The sizes of the loops calculated decrease uniformly while the measured transfer function shows a small loop followed by a large one. Also in the same figure the calculated spiral is seen to be symmetric about the imaginary axis whereas the measured transfer function is seen to be symmetric about a line parallel to the imaginary axis on the positive real side. An aspect of the theory 1 curve and the data that are in agreement is the appearance of loops.

The relation is now shown between Eq. (13) and the theory 1 curve in Figs. 3(c) and (d). The spi-

ral shown in Fig. 3(c) is generated by the term

$$\frac{x_3 e^{-x_1 s}}{1 + x_3 x_2 x_1 s} \quad (15)$$

The decrease in amplitude occurs because the magnitude of

$$\frac{x_3}{1 + x_3 x_2 x_1 s} \quad (16)$$

decreases with frequency.

The change in phase angle with frequency is seen as a rotation in Figs. 3(c) and (d). The rotation is due to a gentle change in phase angle from Eq. (16) combined with a rapid change in phase angle due to the term

$$e^{-x_1 s} \quad (17)$$

The addition of the imaginary term

$$x_4 s \quad (18)$$

to term (15) causes the spiral to be pulled up along the imaginary axis. This effect produces the loops seen in the theory 1 curve of Fig. 3(d). Theory 1 can be modified. The next sections discuss one type of modification.

Theory 2. - As an example of one step in the iteration procedure, the results obtained by modifying the previous model to include the effect of wall storage on the heat transfer process are discussed. The wall storage modification is typical of a modification that can usually be made from a more detailed analysis of the physical processes in a system.

The modification results in a change in the definition of QUA. This modification will be called theory 2. The modified term was

$$QUA_2 = \mu e^{-\lambda} + 1 - \mu \quad (19)$$

where

$$\mu = 1 + \frac{x_1 s (1 - x_{13}/x_{11})}{1 + x_{12}/x_{11} + x_1 s/x_{11}} \quad (20)$$

$$\lambda = \frac{x_1 s + x_{12} - x_{12}}{1 + x_1 s/x_{11}} \quad (21)$$

Thus, using Eqs. (12), (6a), (6d), and (19) yields

$$Z_{1A} = \frac{(\mu e^{-\lambda} + 1 - \mu) x_3}{1 + x_1 x_2 x_3 s} + x_4 s \quad (22)$$

A range of parameter values for x_{11} , x_{12} , and x_{13} was selected. Also, values of the coefficients for the specific operating condition of the example was chosen. The resulting transfer function is shown in Figs. 3(e) and (f).

Examination of Fig. 3(e) shows that the theory 2 curve describes the data at low frequencies as well as the theory 1 curve. The procedure used has minimized the performance index. Still, a

glance at Fig. 3(f) indicates that the theory is not successful since the resulting curve does not resemble the data at high frequencies. The theory 2 loops decrease in size rapidly as the frequency increases. Also, no small loop followed by a large one occurs. This modification is an example of how the extension along well known lines of an idea may result in an unsuccessful transfer function. The final version is discussed next.

Theory 3. - The model found to represent the high vapor exit quality data best consisted of the following set of subsystem transfer functions:

$$QUA = e^{-x_1 s} \quad (23)$$

$$E = x_1 s + \frac{s}{1/x_{10} + s/x_9} \quad (24)$$

$$H = x_2 x_1 s e^{-x_5 s} \quad (25)$$

$$F = \frac{x_8 s}{s^2 + x_6 s + x_7^2} \quad (26)$$

The resulting transfer function, which is plotted in Figs. 3(g) and (h), is designated as theory 3. This model has all the important characteristics of the data at all frequencies. The transfer function has the basic spiral shape below 1 hertz (fig. 3(g)). It also has the small loop between 1.6 and 2.5 hertz. And the larger loop between 2.5 and 4 hertz also exists (fig. 3(h)). Furthermore, the high frequency data are symmetric about a line through the real axis. The inertia effect that pulls the data up parallel to the imaginary axis is also apparent.

The transfer function is

$$Z_{1B} = \frac{e^{-x_1 s} x_3}{1 + x_1 x_2 x_3 s e^{-x_5 s} + \frac{x_3 x_8 s}{s^2 + x_6 s + x_7^2}} + \frac{x_4 s + \frac{s}{1/x_{10} + s/x_9}}{1} \quad (27)$$

The appearance of the small loop before the large one (fig. 3(d)) is due to the additional term $F(s)$. The magnitude of the term

$$\frac{x_3}{1 + x_1 x_2 x_3 s e^{-x_5 s} + \frac{x_3 x_8 s}{s^2 + x_6 s + x_7^2}} \quad (28)$$

becomes very small at the frequency where

$$s^2 + x_7^2 = 0$$

This decrease in magnitude causes the loop that occurs between 1.6 and 2.5 hertz to be small. The high frequency data are symmetric about a line through the real axis parallel to the imaginary axis due to the term

$$\frac{s}{1/x_{10} + s/x_9} \quad (29)$$

in $E(s)$. At high frequencies including the term causes $E(s)$ to become

$$E(s) = x_4 s + x_9 \quad (30)$$

In conclusion, it should be noted that before Eq. (27) was determined no equation existed which gave good agreement with the form of the high vapor exit quality data for the frequency range above 1 hertz.

The three theoretical models used in the study of the high vapor exit quality example are summarized in table 1. The set of coefficients that were obtained using the method with each model and the data are given in table 2. Some additional results of the study are presented next.

Low Quality Vapor Exit Condition

Another result of this study was the discovery that a modification of one term in Eq. (27) would enable that equation to be used to interpret the inlet impedance data taken at a condition of low vapor exit quality. The modification was to use the following form of $F(s)$ instead of Eq. (26).

$$F(s) = \frac{s x_3}{1 + s x_{11}}$$

The excellent agreement possible with this transfer function is demonstrated for a typical low vapor exit quality (20 percent) case⁽²⁾ (case 1) in Fig. 4 where a comparison of the measured and calculated boiler inlet impedance is made.

The procedure described in the report enabled a determination of the transfer function form to be made for low exit vapor quality and high vapor exit quality. Thus it has proved to be valuable in extending and increasing the understanding of the dynamics of boilers.

Concluding Remarks

The search technique used permitted the parameters which were derived from the most certain theoretical aspects of the problem to stay relatively unchanged during the search for a minimum of S_p . A good example was the term x_3 which is calculated from the slope of the pressure drop against flow curve.⁽¹¹⁾ This term determined the magnitude of the transfer function at low frequencies, and it varies by less than 2 percent in a typical computer calculation.

The parameters which were less certain took on a larger range of values during a search. The difficulty is that the Powell method generally provides only a local minimum and this means that the solution is not inherently unique. The theoretical results are still considered valid since they apply to a range of experiments with different steady-state conditions and boiler geometries. The value of the constants obtained are also physically reasonable since the use of penalty functions provides estimates which are possible.

Appendix - Symbols

A	cross-sectional area of boiler tube, m^2
d	constraint on value of transfer function constant
$E(s)$	subsystem transfer function
$F(s)$	subsystem transfer function
f	frequency, Hz
$G(s)$	subsystem transfer function
$H(s)$	subsystem transfer function
I	inertia, sec
j	$\sqrt{-1}$
k	gain
\bar{L}_{sc}	subcooled length, m
$\Delta L_{sc}/\bar{L}_{sc}$	perturbation in subcooled length
P	pressure, N/m^2
\bar{P}	mean pressure, N/m^2
$\Delta P/\bar{P}$	perturbation in pressure
p	penalty function
R	subsystem transfer function
S	performance measure
S_p	penalized performance measure
S_w	weighted performance measure
s	Laplace operator, sec^{-1}
T	time delay, sec
W	mass flow, kg/sec
\bar{W}	mean mass flow, kg/sec
$\Delta W/\bar{W}$	perturbation in mass flow
w	weighting factor in penalty function
{x}	set of transfer function constants
Z	transfer function
$\bar{Z} = (\bar{P}/\bar{W})$	impedance value relative to which all transfer functions are compared, scale factor 3.28×10^6 (n-sec/ $m^2 kg$) ⁻¹
α	weighting factor in performance measure
δ	weighting factor for penalty

References

1. Krejsa, E. A., Goodykoontz, J. H., and Stevens, G. H., "Frequency Response of Forced-Flow Single-Tube Boiler," TN D-4039, 1967, NASA, Cleveland, Ohio.
2. Goodykoontz, J. H., Stevens, G. H., and Krejsa, E. A., "Frequency Response of Forced-Flow Single-Tube Boiler with Inserts," TN D-4189, 1967, NASA, Cleveland, Ohio.
3. Stevens, G. H., Krejsa, E. A., and Goodykoontz, J. H., "Frequency Response of a Forced Flow Single Tube Boiler with Inserts and Exit Restrictions," TN D-5023, 1969, NASA, Cleveland, Ohio.
4. Law, V. J. and Bailey, R. V., "A Method for the Determination of Approximate System Transfer Functions," Chemical Engineering Science, Vol. 18, Mar. 1963, pp. 189-202.
5. Bellman, R., Kagiwada, H., and Kalaba, R., "Identification of Linear Systems Via Numerical Inversion of Laplace Transforms," RM-4262-PR, AD-444517, Aug. 1964, Rand Corp., Santa Monica, Calif.
6. Meditch, J. S. and Stoll, P. J., "On Respiratory System Parameter Estimation," 11th Joint Automatic Control Conference, ASME, 1970, pp. 383-390.
7. Pierre, D. A., Optimization Theory with Applications, John Wiley & Sons, Inc., 1969.
8. Powell, M. J. D., "An Efficient Method for Finding the Minimum of a Function of Several Variables Without Calculating Derivatives," Computer Journal, Vol. 7, 1964, pp. 155-162.
9. Shapiro, M. S. and Goldstein, M., "A Collection of Mathematical Computer Routines," AEC-NYO-1480-14, Feb. 1965, New York Univ., New York, N.Y.
10. Dorf, R. C., Modern Control Systems, Addison-Wesley Publ. Co., 1967.
11. Krejsa, E. A., "Model for Frequency Response of a Forced Flow, Hollow, Single Tube Boiler," TM X-1528, 1968, NASA, Cleveland, Ohio.

TABLE 2. - DIMENSIONLESS TRANSFER FUNCTION

GAINS^a AND TIME CONSTANT PARAMETERS

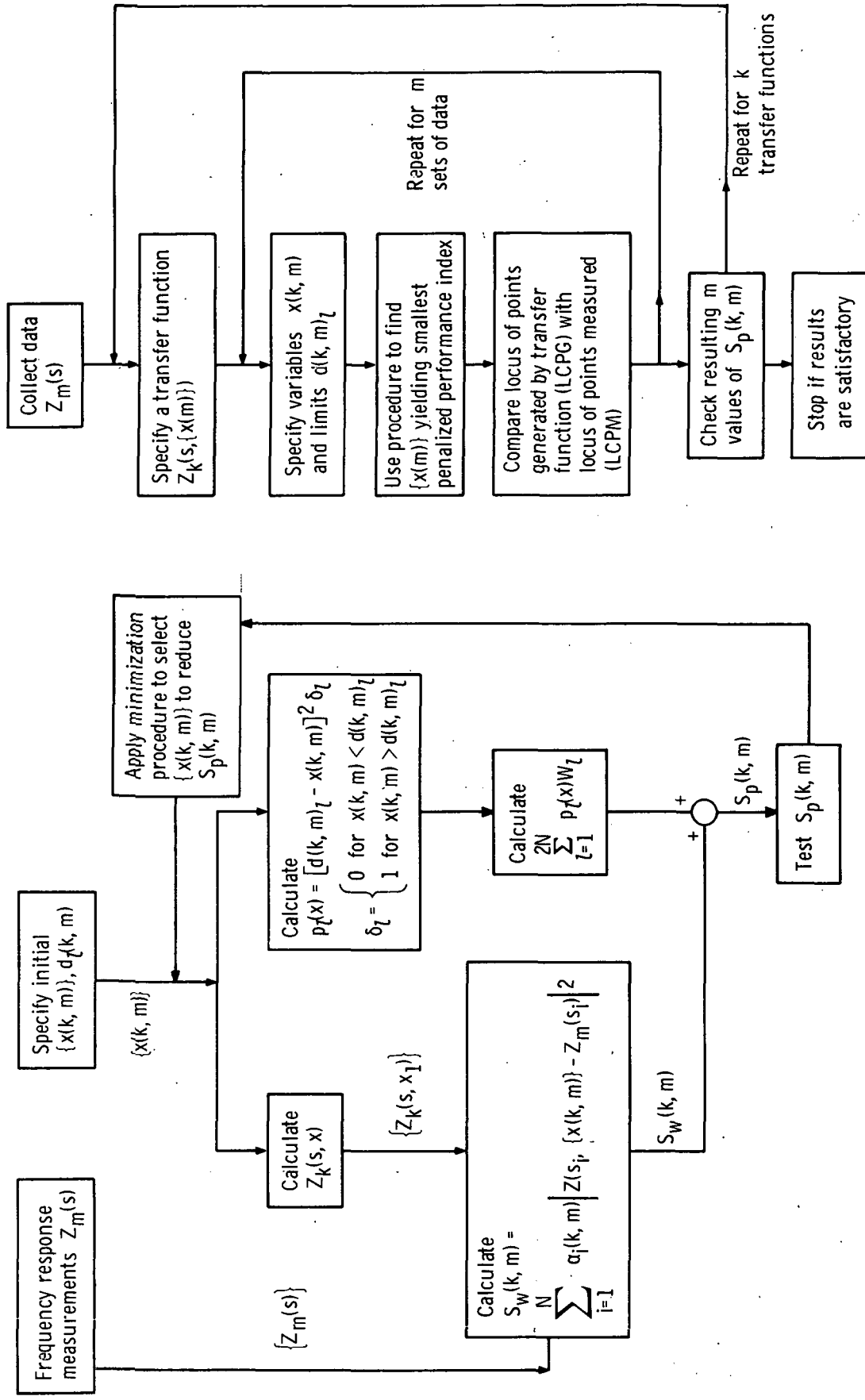
Transfer function parameter	Theory		
	1	2	3
x_1 , sec	0.794	0.706	0.883
x_2	1.96	1.72	0.44
x_3	0.855	0.881	0.845
x_4 , sec	1.00×10^{-2}	5.00×10^{-3}	0.00296
x_5 , sec	-----	-----	0.174
x_6 , sec ⁻¹	-----	-----	2.01
x_7 , sec ⁻¹	-----	-----	12.8
x_8 , sec ⁻¹	-----	-----	138.0
x_9	-----	-----	0.0365
x_{10} , sec	-----	-----	0.098
x_{11}	-----	190.0	-----
x_{12}	-----	3.06	-----
x_{13}	-----	1.46	-----

^aGains relative to 3.28×10^6 N-sec/m²-kg.

TABLE 1. - COMPARISON OF FUNCTIONAL FORMS
OF TRANSFER FUNCTION TERMS
FOR DIFFERENT THEORIES

$$\begin{aligned} \mu &= 1 + x_1 s (1 - x_{13}/x_{11}) / (1 + x_{12}/x_{11} + x_1 s/x_{11}); \\ \lambda &= x_1 s + x_{12} - x_{12}/(1 + x_1 s/x_{11}) \end{aligned}$$

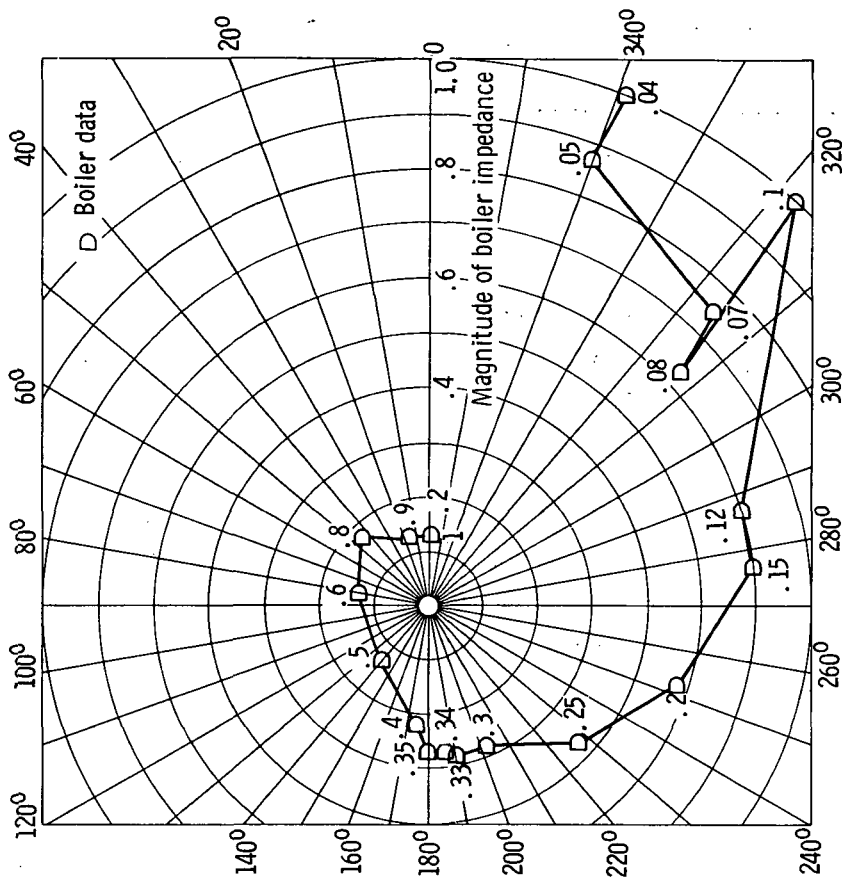
Transfer function term	Theory		
	1	2	3
QUA	$e^{-x_1 s}$	$\mu e^{-\lambda} + 1 - \mu$	$e^{-x_1 s}$
E	$x_4 s$	$x_4 s$	$x_4 s + s/(1/x_{10} + s/x_9)$
H	$x_2 x_1 s$	$x_2 x_1 s$	$x_2 x_1 s e^{-x_5 s}$
F	0	0	$x_6 s / (s^2 + 2s x_6 + x_7^2)$

(a) Procedure used to check transfer function $Z_k(s, x)$.

(b) Procedure used to find a satisfactory transfer function.

Figure 1. - Flow charts illustrating identification procedures.

Figure 1. - Concluded.



(a) Boiler data for frequencies below 1 hertz.

Figure 3. - Comparison of boiler data and experimental models for condition of 99 percent vapor exit quality (ref. 2, run 4). (Impedance relative to $3.28 \times 10^6 \text{ N-sec/m}^2\text{-kg.}$) Note: To avoid confusion and increase graphical clarity, frequency calculated from the theories was not shown on the curves. While judging agreement in magnitude is possible; judging agreement in phase angle is not. To see that at all frequencies it is possible to achieve good agreement of the phase angle and magnitude for the data and the calculations based on theory 3, see figures 4 and 5. Phase and magnitude for curves based on theories 1 to 3 in this figure agreed with the data at frequencies up to 1 hertz; beyond 1 hertz only theory 3 shows good agreement.

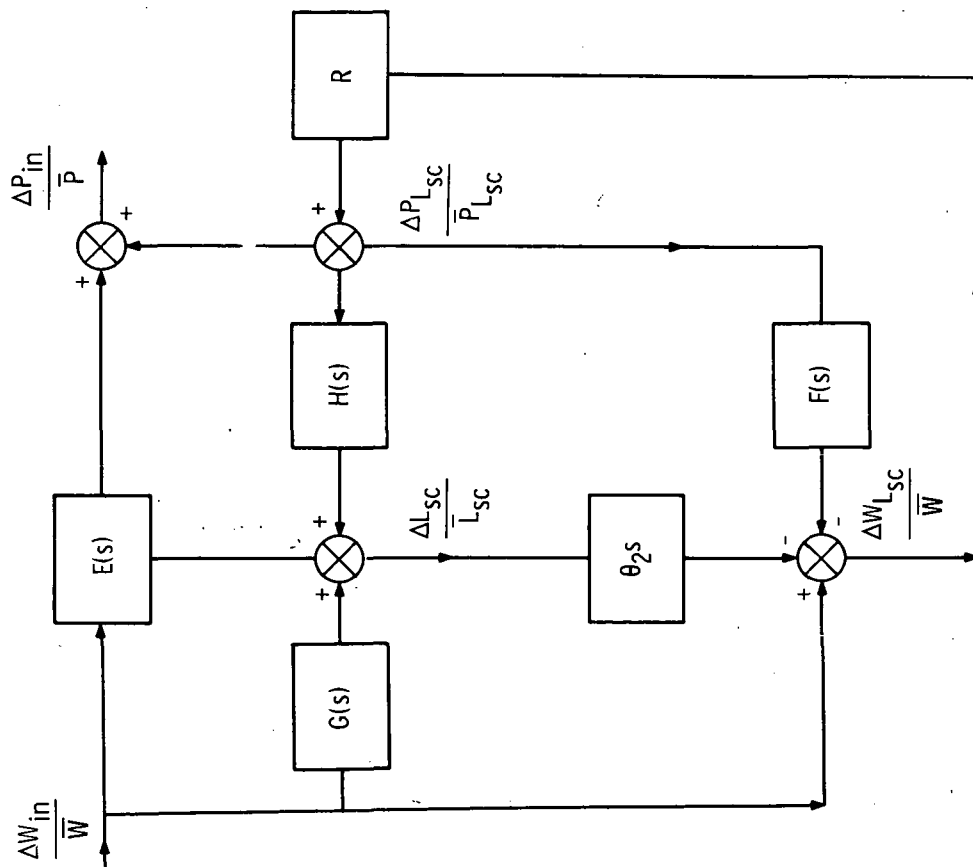
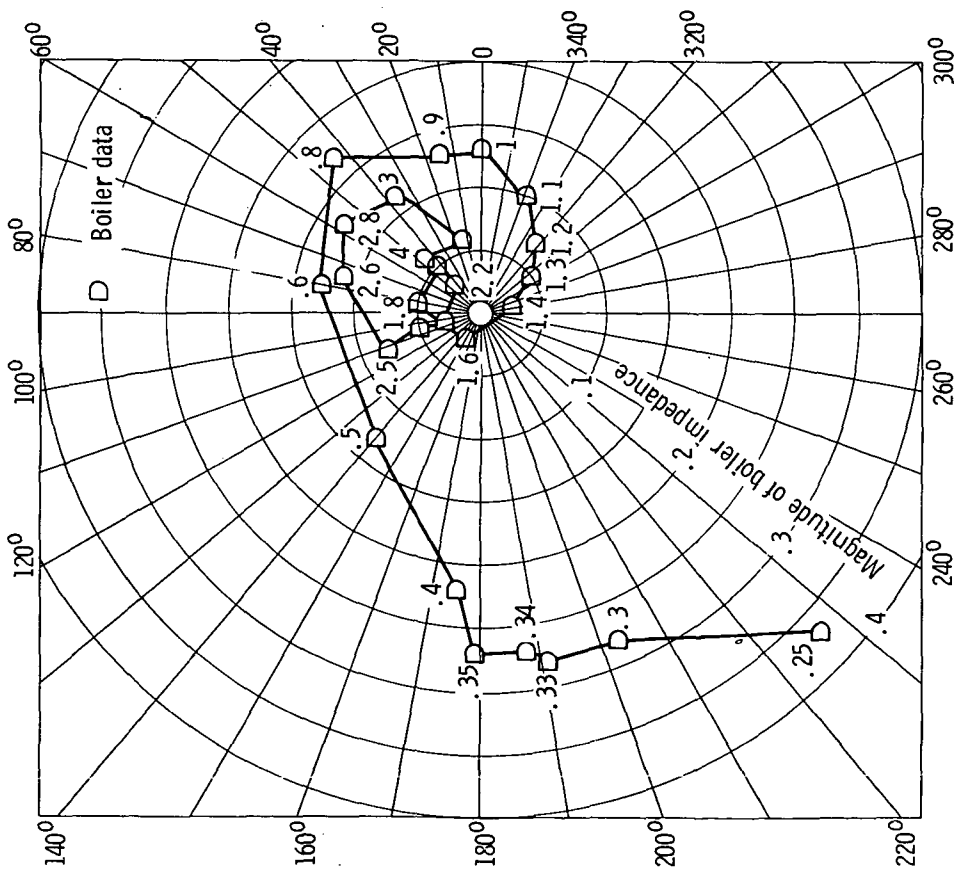
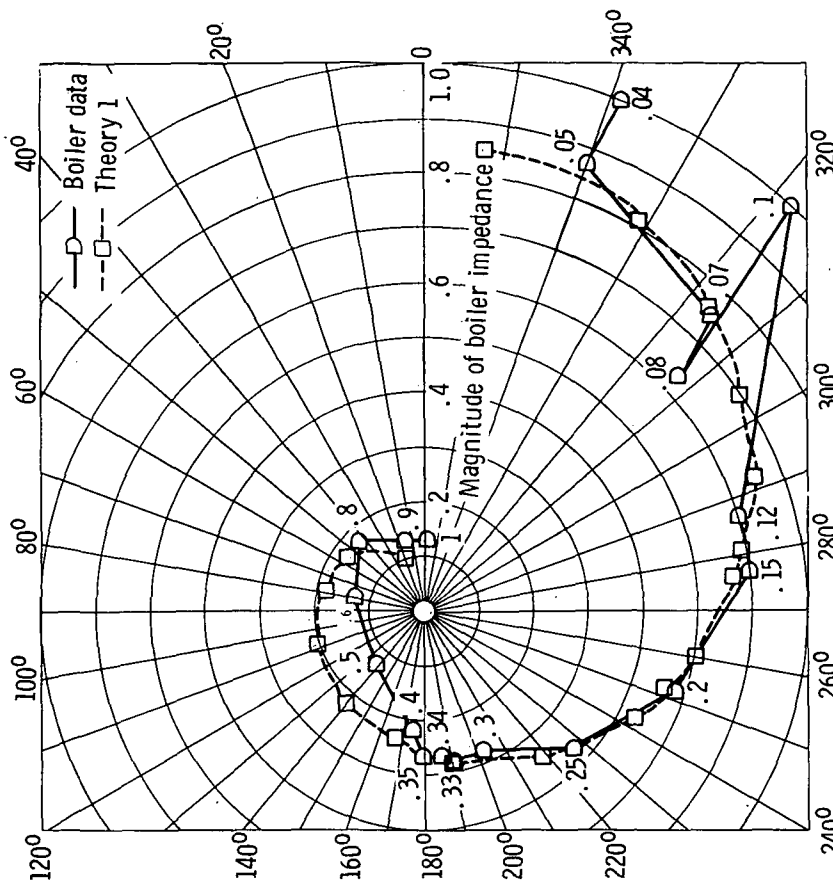


Figure 2. - Block diagram of system.



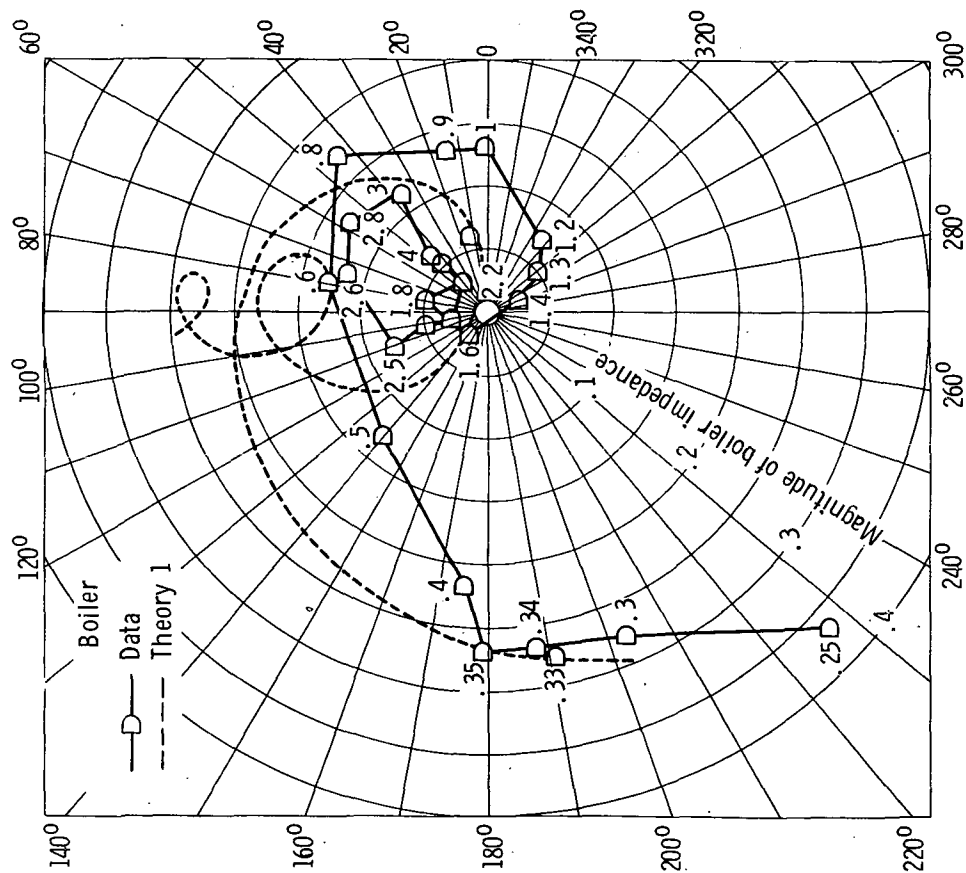
(b) Boiler data for frequencies above 0.25 hertz.

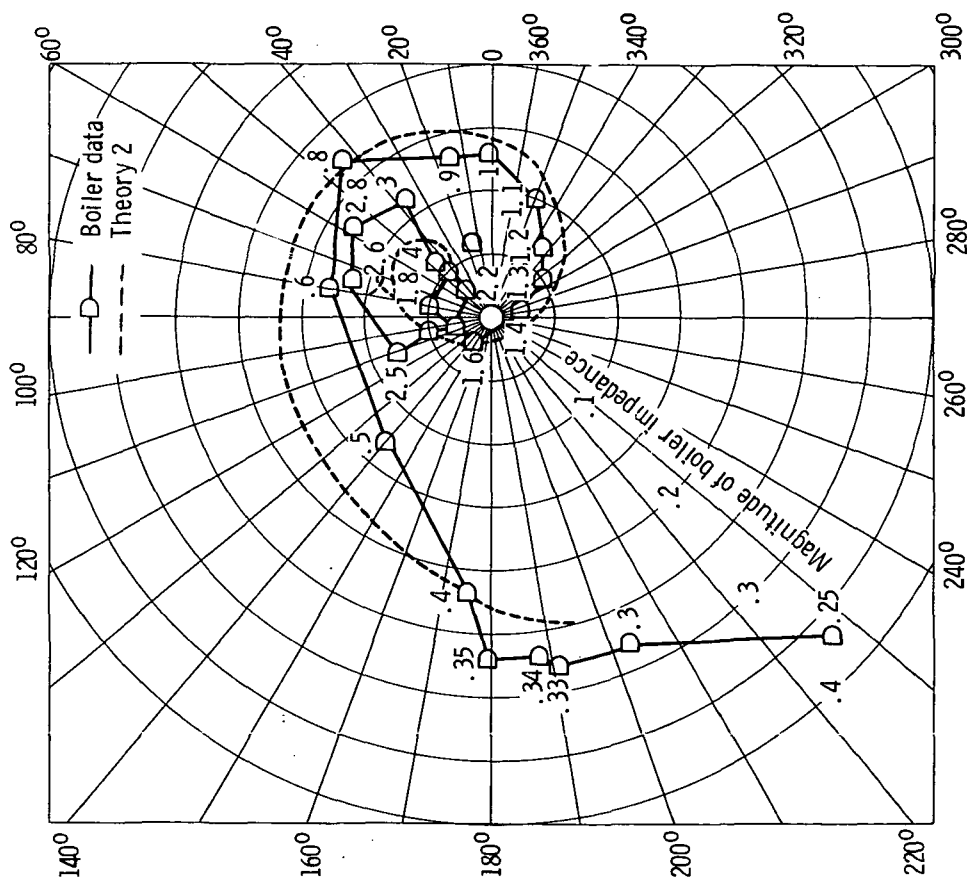
Figure 3. - Continued.



(c) Comparison of boiler data and theory 1 at frequencies below 1 hertz.

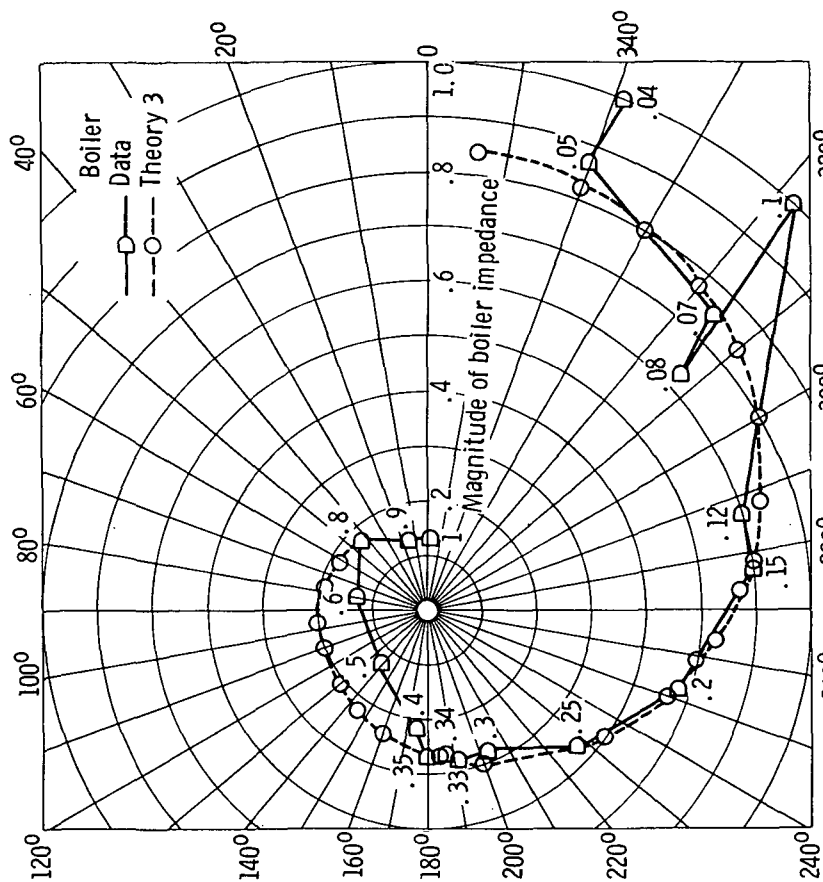
Figure 3. - Continued.





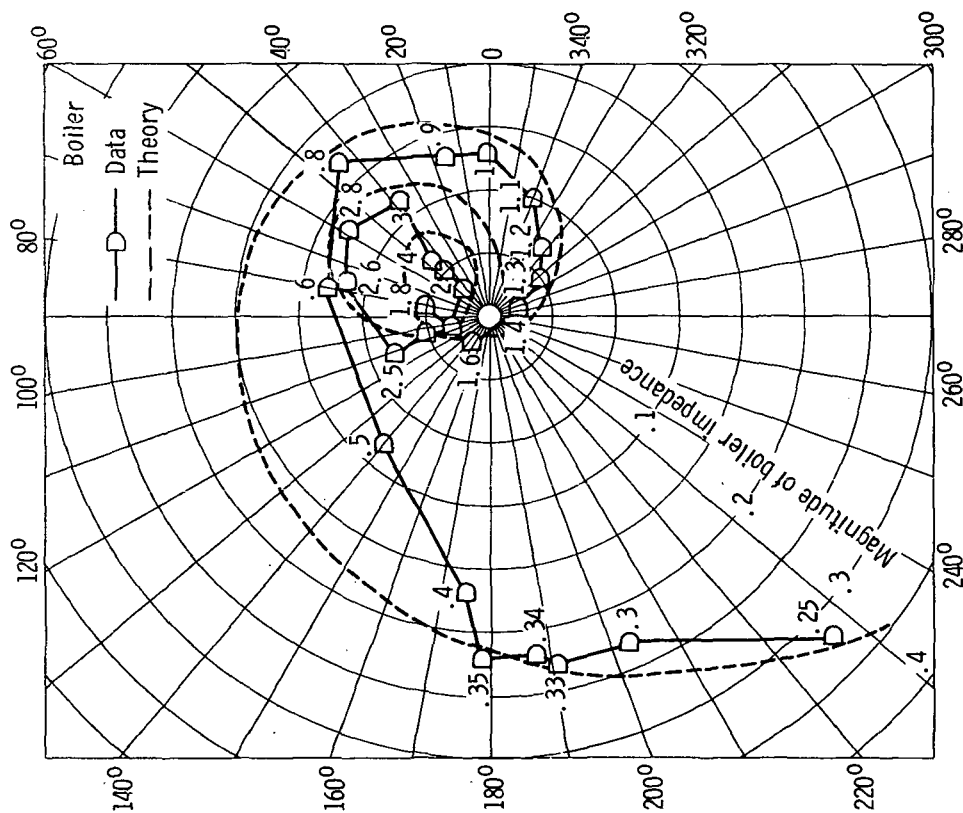
(f) Comparison of data and theory 2 for frequencies above 0.3 hertz.

Figure 3. - Continued.



(g) Comparison of boiler data and theory 3 at frequencies below 1.0 hertz.

Figure 3. - Continued.



(h) Comparison of boiler data and theory 3 for frequencies above 0.3 hertz.

Figure 3. - Concluded.

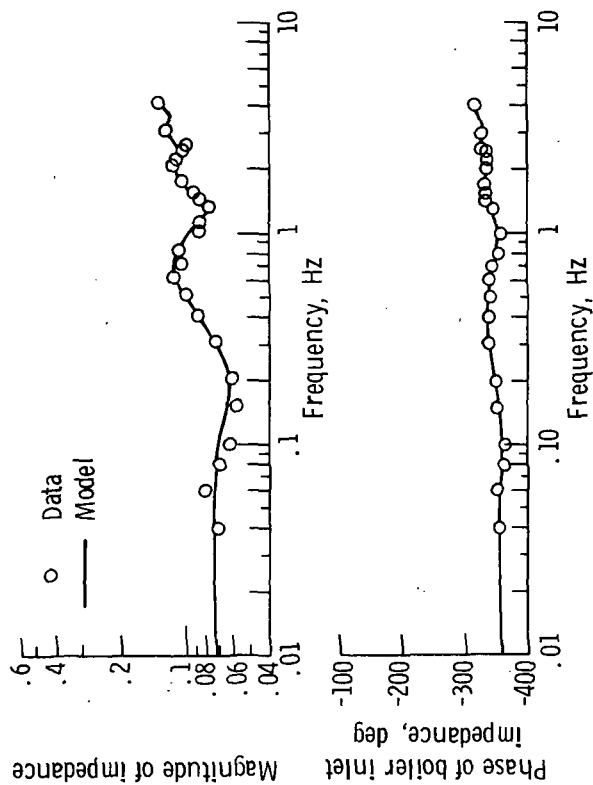


Figure 4. - Comparison of experimental data and calculated boiler inlet impedance for exit condition of 20 percent vapor exit quality (ref. 2, run 1). (Impedance relative to 3.2×10^6 N-sec/m²-kg.)